



Electron momentum distribution and electronic response of ceramic borides



N.L. Heda^a, B.S. Meena^b, H.S. Mund^b, Jagrati Sahariya^c, Kishor Kumar^b, B.L. Ahuja^{b,*}

^a Department of Pure and Applied Physics, University of Kota, Kota 324005, India

^b Department of Physics, Mohanlal Sukhadia University, Udaipur 313001, India

^c Department of Physics, Manipal University, Jaipur 303007, India

ARTICLE INFO

Keywords:

X-ray scattering
Ceramic compounds
Density functional theory

ABSTRACT

Isotropic Compton profiles of transition metal based ceramics TaB and VB have been measured using ¹³⁷Cs (661.65 keV) γ -ray Compton spectrometer. The experimental momentum densities are compared with those deduced using linear combination of atomic orbitals (LCAO) with Hartree-Fock (HF), density functional theory (DFT) with Wu-Cohen generalized gradient approximation (WCGGA) and also the hybridization of HF and DFT (namely B3PW and PBE0) schemes. It is found that LCAO-DFT-WCGGA scheme based profiles give an overall better agreement with the experimental data, for both the borides. In addition, we have computed the Mulliken's population (MP) charge transfer data, energy bands, density of states and Fermi surface topology of both the borides using full potential-linearized augmented plane wave (FP-LAPW) and LCAO methods with DFT-WCGGA scheme. Cross-overs of Fermi level by the energy bands corresponding to B-2p and valence d-states of transition metals lead to metallic character in both the compounds. Equal-valence-electron-density profiles and MP analysis suggest more ionic character of VB than that of TaB.

1. Introduction

Compton scattering (CS) is useful technique to explore the reliability of ground state electronic wave functions of the target materials [1–3]. Within the criteria of impulse approximation, the double differential scattering cross-section is directly related to the Compton profile (CP), $J(p_z)$, and hence the electron momentum density, $n(\mathbf{p})$. Mathematically,

$$\frac{d^2\sigma}{d\Omega d\omega_2} \propto J(p_z) = \iint n(\mathbf{p}) d^3p, \quad (1)$$

where X-ray scattering vector lies along the z-axis and ω_2 is the scattered photon energy. Further, the $n(\mathbf{p})$ is related to electron wave function in real space.

Transition metal borides based on V, Nb and Ta are known as important ceramics due to their peculiar physical and chemical properties, like high hardness, high electrical and thermal conductivity, chemical stability and good corrosion resistance [4–7]. Particularly, the phase diagrams of V-B and Ta-B systems show six boride phases (VB, VB₂, V₂B₃, V₃B₂, V₃B₄, V₅B₆ and TaB, TaB₂, Ta₂B, Ta₃B₂, Ta₃B₄, Ta₅B₆) [8–11]. Structural, mechanical and electronic properties of TaB₂ and TaB have been studied by Zhao

and Wang [8] using density functional theory (DFT) within projector-augmented-wave (PAW) method. The elastic properties, electronic structure and thermodynamic behavior of TaB have been investigated by Chen et al. [12] using first-principles plane-wave ultrasoft-pseudopotential scheme within CASTEP code. Yao et al. [13] have carried out DFT calculations to understand the structural and electronic properties of transition metal borides. Further, Qi et al. [14] have reported the stability, chemical bonding, elastic constants, hardness and Debye temperature of VB, NbB and TaB using DFT calculations.

In this paper, we report CP measurements of TaB and VB using 20 Ci ¹³⁷Cs Compton spectrometer [15,16]. The isotropic experimental CPs have been used to validate various exchange and correlation potentials within linear combination of atomic orbitals (LCAO) method [17]. Further, we have also employed LCAO and full potential-linearized augmented plane wave (FP-LAPW) method [18] to deduce the Mulliken's population (MP), energy bands, density of states (DOS) and Fermi surfaces (FSs) of both the borides. In addition, the relative nature of bonding in TaB and VB has also been discussed using MP analysis and after scaling the theoretical and experimental Compton data to equal-valence-electron-density (EVED).

* Corresponding author.

E-mail address: blahuja@yahoo.com (B.L. Ahuja).

2. Methodology

2.1. Experiment

The CP measurements were performed using an indigenous 740 GBq (20 Ci) ^{137}Cs γ -ray Compton spectrometer [15,16]. In individual experiments, high purity ($\geq 99.99\%$) polycrystalline powders of TaB and VB were pressed to form pellets of diameter 2.56 and thickness 0.43 cm. The incident γ -rays (661.65 keV) were scattered at an angle of $160 \pm 0.6^\circ$ from the sample and detected by high purity Ge detector (Canberra, Model GL0510P) and associated electronics. Here, the Ge crystal has the cross-section of 500 mm² with 10 mm thickness. The momentum resolution (Gaussian full-width at half maximum, FWHM) of the spectrometer (which includes detector response and instrumental broadening) was 0.34 a.u. During the experiment, the stability of the detection system was checked from time-to-time using ^{57}Co and ^{133}Ba calibration sources. To accumulate the raw data, the sample TaB (VB) was exposed for 332 (133) h leading to 1.3×10^5 (0.65×10^5) integrated counts in the CP region. The background (BG) was measured for 93 h, in the absence of sample in the sample-holder. Before subtraction of BG from the raw data, the BG was scaled to measurement time of raw Compton data. To deduce true CP, the raw Compton data were corrected for a series of systematic corrections, like background, detector response (limited to stripping-off the low energy tail), sample absorption, Compton cross-section and multiple scattering, etc. using the methodology developed by Warwick group [19,20]. The experimental profiles were normalized to corresponding free-atom CP area [21] as discussed in the next section.

2.2. Theory

2.2.1. LCAO method

The energy bands, partial and total DOS, MP charge transfer data and CPs of TaB and VB have been derived using LCAO method as embodied in CRYSTAL09 code [17]. In the LCAO technique, each crystalline orbital is derived from the linear combination of Bloch functions and the local functions are constructed from the Gaussian-type basis sets. In the present calculations, we have used HF, generalized gradient approximation (GGA) within DFT and the hybridization of HF to DFT (B3PW and PBE0 schemes). In such calculations, one solves the following Schrodinger equation,

$$\left[\hat{H}_{\text{HF/DFT}} = \hat{i} + \hat{v} + \hat{J}[n(\vec{r})] + \hat{K}_{\text{HF}}[n(\vec{r}, \vec{r}')] \right] \frac{\partial E_{\text{xc}}[n(\vec{r})]}{\partial n(\vec{r})} \phi_i(\vec{r}) = \epsilon_i \phi_i(\vec{r}). \quad (2)$$

In Eq. (2), \hat{i} , \hat{v} , \hat{J} , \hat{K}_{HF} and E_{xc} represent the operators for kinetic energy of electrons, external potential, Coulomb, nonlocal exchange energy and exchange-correlation density functional energy, respectively. In the DFT-GGA, B3PW and PBE0 schemes, the E_{xc} is defined in the following sequence,

$$E_{\text{XC}}[n(\vec{r})] = \int n(\vec{r}) \varepsilon_{\text{XC}}[n(\vec{r}), |\vec{\nabla} n(\vec{r})|] d\vec{r} \quad (3)$$

$$E_{\text{XC}}^{\text{B3PW}} = 0.80 \times E_{\text{X}}^{\text{LDA}} + 0.72 \times \Delta E_{\text{X}}^{\text{BECKE}} + 0.20 \times E_{\text{X}}^{\text{HF}} + 0.19 \times E_{\text{C}}^{\text{VWN}} + 0.81 \times E_{\text{C}}^{\text{PWGGA}} \quad (4)$$

$$E_{\text{XC}}^{\text{PBE0}} = 0.25 \times E_{\text{X}}^{\text{HF}} + 0.75 \times E_{\text{X}}^{\text{PBE}} + E_{\text{C}}^{\text{PBE}} \quad (5)$$

In case of HF, only exchange potential is considered [17] while correlation effects are neglected. For the modeling of computation under DFT-GGA, exchange energy prescribed by Wu and Cohen [22] and correlation energy given by Perdew et al. [23] have been considered, which are referred as DFT-WCGGA in the forthcoming discussion. For the E_{X}^{HF} , $E_{\text{X}}^{\text{LDA}}$, $\Delta E_{\text{X}}^{\text{BECKE}}$ and $E_{\text{X}}^{\text{PBE}}$ the exchange energies of HF [17], Dirac-Slater [17], with Becke gradient [24] and Perdew et al. [23], respectively, are considered. Correlation energies $E_{\text{C}}^{\text{PBE}}$, $E_{\text{C}}^{\text{VWN}}$ and $E_{\text{C}}^{\text{PWGGA}}$ are taken from the formulations, suggested by Perdew et al.

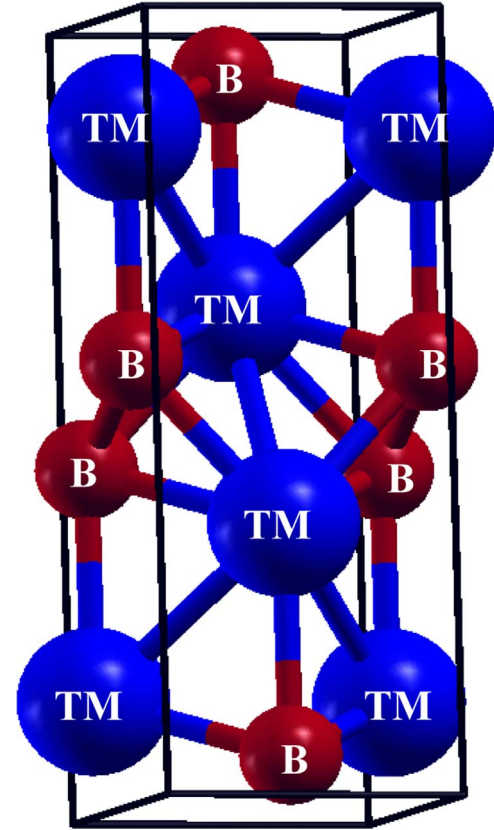


Fig. 1. Structural sketch of hexagonal TMB (TM=Ta or V) computed using the XCrystal software of Kokalj [27].

[23], Vosko-Wilk-Nusair [25] and Perdew and Wang [26], respectively. Due to the non-availability of all-electron basis sets of Ta, we have employed pseudo-potential basis sets for Ta, while in case of V and B all-electron basis sets were taken (website www.tcm.phy.cam.ac.uk). Using Billy software [17], the basis sets were optimized for minimum possible energy for both the borides. The integration in the reciprocal space has been carried out on a grid of 512 \mathbf{k} points in the irreducible Brillouin zone (BZ). To derive the absolute (total) CPs, we have added the corresponding free-atom core contribution [21] to the present isotropic and anisotropic LCAO valence profiles. The absolute theoretical profiles for TaB and VB were normalized to corresponding Hartree-Fock (HF) free-atom CPs area [21] viz. 29.39 and 13.49 e⁻ in the momentum range 0–7 a.u. It is worth mentioning that we have considered $3d^3 4s^2$ ($5d^3 6s^2$) valence electron configuration for VB (TaB) which gives the HF free-atom area 3.99 e⁻ (in the range 0–7 a.u.) for both the samples. The HF free-atom area of core electrons in the momentum range 0–7 a.u. for VB (TaB) was 8.79 (25.40) e⁻ [21].

2.2.2. FP-LAPW method

In addition to LCAO calculations, we have also explored the structural and electronic properties of TaB and VB using the FP-LAPW method [18]. In this full-potential method, there is no shape approximation to the charge density or potential. Looking at the success of WCGGA in predicting the momentum density of both the borides (as discussed later), we have used the exchange and correlation potentials within Wu and Cohen GGA [22] in the FP-LAPW calculations. It is worth mentioning that in FP-LAPW method, the wave function, charge density and potential are well approximated by spherical harmonic functions inside non-overlapping spheres surrounding the atomic sites (muffin-tin, MT, spheres), while a plane wave basis set is used in the residual part of unit cell (interstitial region). The smallest MT radius multiplied by the maximum amplitude of reciprocal lattice vector (\mathbf{K}) in the expansion of plane waves in the

Download English Version:

<https://daneshyari.com/en/article/5492136>

Download Persian Version:

<https://daneshyari.com/article/5492136>

[Daneshyari.com](https://daneshyari.com)